**SUPPLEMENTAL DATA**

**Supplemental Figure 1.** Disruption of autophagic flux in *Atg13* mutants. (**A**) Shown are fixed fat body samples from control and $Atg13^{\Delta 81}$ mutant animals expressing UAS-LAMP-GFP and UAS-mCherry-Atg8a, which label lysosomal and autophagic vesicles, respectively. In control animals, starvation results in a progressive enlargement of LAMP-GFP structures, most of which co-label with mCherry-Atg8a by 4 hours. Disruption of Atg13 blocks both the enlargement of lysosomes and their co-labeling with mCherry-Atg8a. (**B**) $Atg13^{\Delta 81}$ mutant clone (GFP-negative cells) showing accumulation of endogenous P62/Ref(2)P.

**Supplemental Figure 2.** Additional Atg1 and Atg13 autophagy phenotypes. (**A-C**) Atg13 RNAi suppresses starvation-induced autophagy. 4-hr starvation induces punctate GFP-Atg8a staining in control cell clones (A) but not in cells co-expressing the hairpin construct 7331-r1 (B). Clonal expression of 7331-r1 (GFP-positive cells) blocks punctate LysoTracker Red staining in response to starvation (C). (**D**) Rapamycin treatment induces punctate localization of mCherry-Atg8a in control cells of the eye-antennal imaginal disc but not in cell clones mutant for *Atg13* (GFP-negative cells). (**E**) *Atg13* mutant cells (GFP-negative) are resistant to induction of punctate mCherry-Atg8a localization induced developmentally during the wandering L3 (wL3) larval stage. (**F-G**) *Atg1* mutant cell clones (dsRed-negative cells) fail to display punctate GFP-Atg8a staining in response to 4-hr starvation (F) or to developmental cues at the wL3 stage (G). (**H-J**) Nutrient- and Atg1-independent induction of autophagy by activation of Jnk signaling. Overexpression of the Jun kinase homolog Bsk leads to formation of mCherry-Atg8a punctae under fed conditions (I), which is not observed in control animals expressing mCherry-Atg8a alone (H). Expression of Bsk also leads to mCherry-Atg8a punctae in $Atg1^{\Delta 3D}$ homozygous mutant animals (J). (**K-L**) Cell clones overexpressing Atg1 from the GS10979 UAS element in the *Atg1* locus (GFP-positive cells) display weak LysoTracker Red staining in the perinuclear region (K). Co-expression of Atg13 leads to a larger, more intensely staining punctate structures (L).

**Supplemental Figure 3.** Nutrient- and TOR-dependent phosphorylation of Atg1 and Atg13. Shown are immunoblot analyses of fat body tissues dissected from *Drosophila* larvae expressing

Myc-Atg1 or Atg13-Flag and indicated UAS-regulated transgenes, using the hs-GAL4 driver. (**A, D**) Sub-populations of Atg13-Flag (A) and Myc-Atg1 (D) with reduced mobility can be identified under both fed and starved conditions; the upper form of each protein is reduced in response to phosphatase treatment (CIP). Starvation leads to a moderate increase in levels and a more modest change in phosphorylation of both proteins. Phosphorylation of kinase-defective (KD) Myc-Atg1 is apparent only under fed conditions. (**B, E**) Overexpression of Rheb or Tsc1/Tsc2 mimics the effects of nutrient signaling, leading to a slight increase in the effect of feeding (Rheb) or starvation (Tsc1/2) on Atg13-Flag (B) and Myc-Atg1 (E) phosphorylation. (**C**) Effect of nutrient status and TOR activity on Atg13-Flag phosphorylation in later stage (96-120 hr @ 25 °C) larvae. Under these conditions, co-expression of Atg1 stimulates phosphorylation of Atg13-Flag under both fed and starved conditions. Co-expression of Tsc1/Tsc2 inhibits the nutrient-dependent phosphorylation, whereas Rheb has little effect. (**F**) Comparison of protein expression levels of UAS-Atg1 transgenic lines. Immunoblot of fat body extracts from equal numbers of larvae expressing either Myc-tagged Atg1, untagged Atg1 from a pUAST-Atg1 transgene (6B) or untagged Atg1 from a GAL4-responsive construct inserted in the Atg1 locus (GS10797), probed with affinity-purified rabbit antibodies raised against the C-terminal 20 residues of *Drosophila* Atg1. These antibodies detect overexpressed wild type and epitope tagged Atg1, but not the endogenous protein, as indicated by the lack of bands corresponding to non-tagged Atg1 in lanes 1 and 2.

**Supplemental Figure 4.** Requirement for Atg13 in Atg1 overexpression phenotypes. (**A, B**) *Atg13* mutation suppresses Atg1-induced apoptosis. Constitutive overexpression of Atg1 throughout the larval fat body was mediated by Cg-GAL4 and UAS-Atg1$^{GS10797}$ transgenes. In control animals, Atg1 overexpression results in reduced organ size and extensive cell death, as indicated by the presence of TUNEL-positive, highly condensed nuclei (A). No TUNEL-positive nuclei were observed in *Atg13* mutants overexpressing Atg1 (B). (**C, D**) Loss of Atg13 does not suppress the cell size reduction caused by high levels of Atg1. Clonal overexpression of Atg1 using Act>CD2>GAL4 and UAS-Atg1$^{6B}$ inhibits cell growth in both control (C) and Atg13 mutant (D) animals. GFP marks Atg1 expressing cells; cell boundaries are labeled by phalloidin.

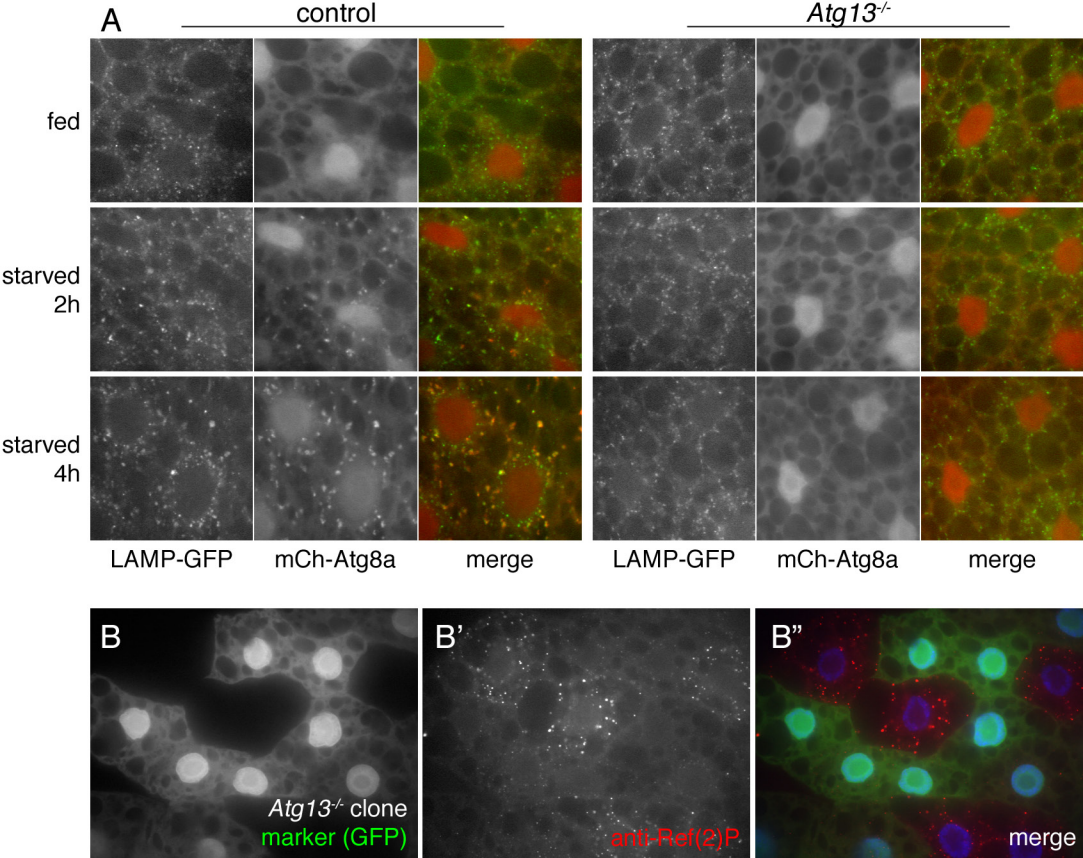
A
control
Atg13-/-
fed
starved 2h
starved 4h
LAMP-GFP
mCh-Atg8a
merge
LAMP-GFP
mCh-Atg8a
merge
B
Atg13-/- clone
marker (GFP)
B'
anti-Ref(2)P
B"
merge

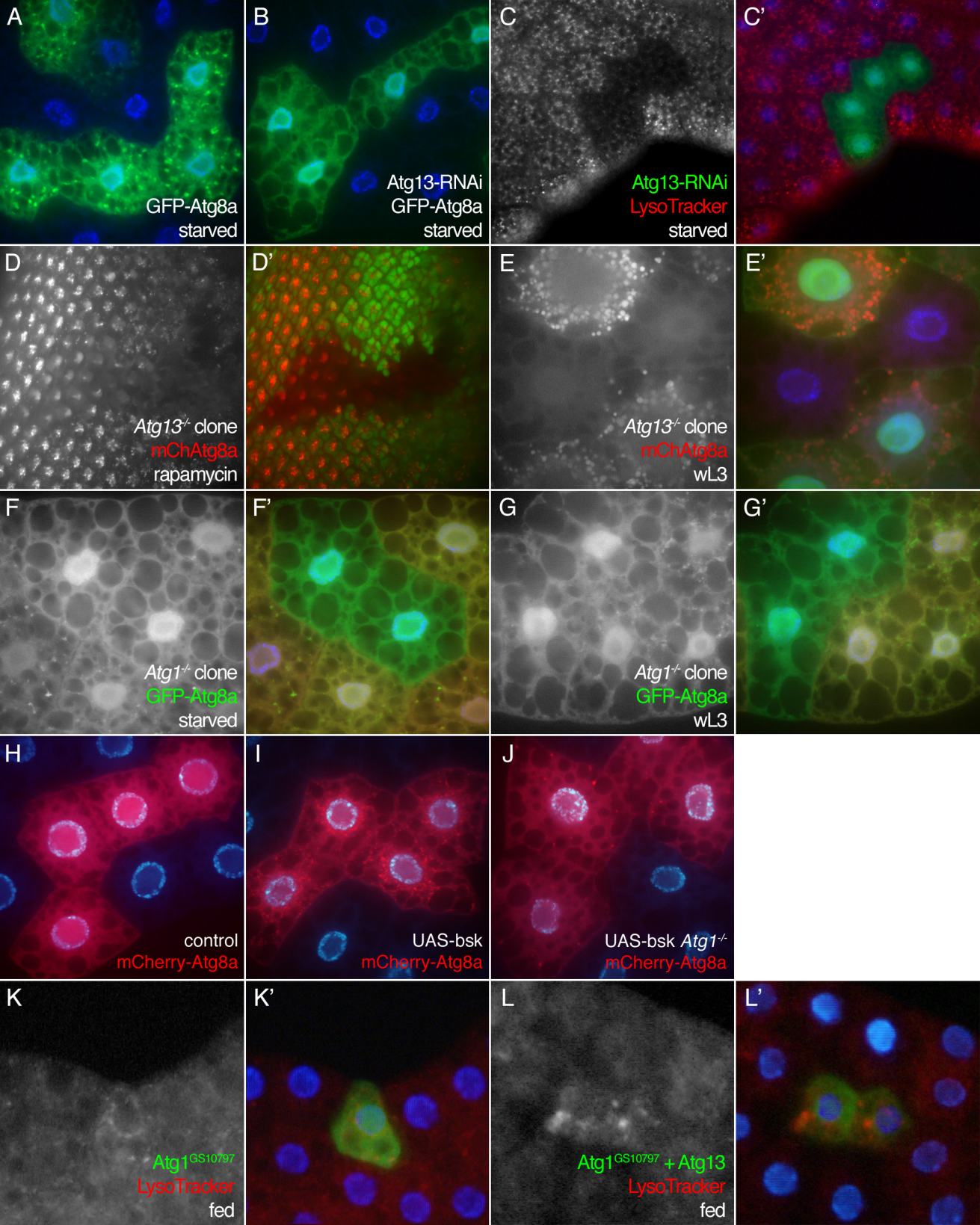
A
GFP-Atg8a
starved
B
Atg13-RNAi
GFP-Atg8a
starved
C
Atg13-RNAi
LysoTracker
starved
C'
D
Atg13-/- clone
mChAtg8a
rapamycin
D'
E
Atg13-/- clone
mChAtg8a
wL3
E'
F
Atg1-/- clone
GFP-Atg8a
starved
F'
G
Atg1-/- clone
GFP-Atg8a
wL3
G'
H
control
mCherry-Atg8a
I
UAS-bsk
mCherry-Atg8a
J
UAS-bsk Atg1-/-
mCherry-Atg8a
K
Atg1GS10797
LysoTracker
fed
K'
L
Atg1GS10797 + Atg13
LysoTracker
fed
L'

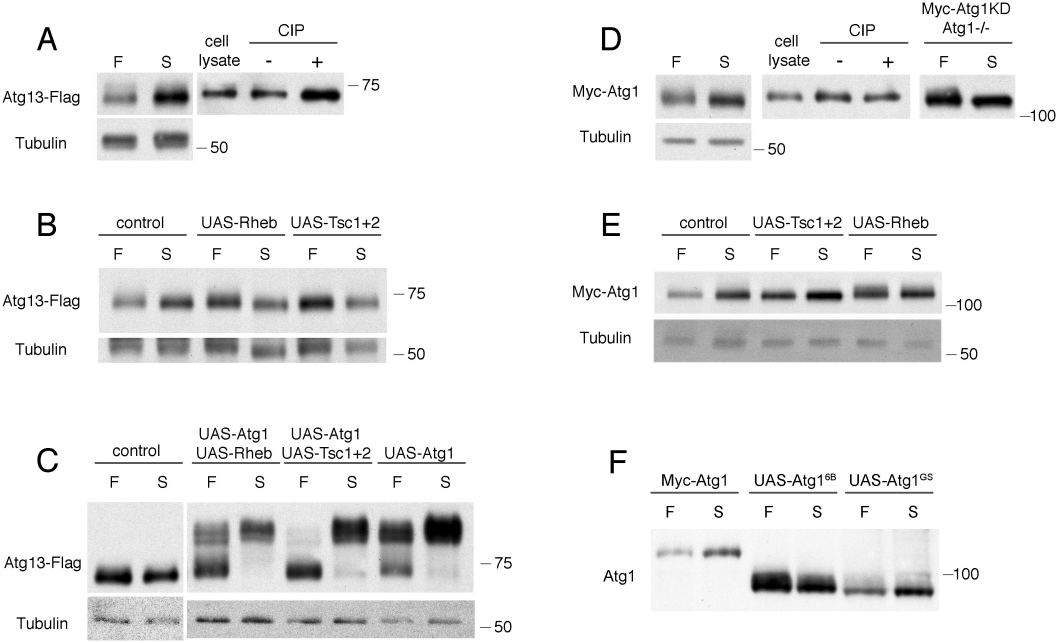
A
F
S
cell lysate
CIP
-
+
Atg13-Flag
Tubulin
75
50
B
control
UAS-Rheb
UAS-Tsc1+2
F
S
F
S
F
S
Atg13-Flag
Tubulin
75
50
C
control
UAS-Atg1 UAS-Rheb
UAS-Atg1 UAS-Tsc1+2
UAS-Atg1
F
S
F
S
F
S
F
S
Atg13-Flag
Tubulin
75
50
D
Myc-Atg1KD Atg1-/-
F
S
cell lysate
CIP
-
+
F
S
Myc-Atg1
Tubulin
100
50
E
control
UAS-Tsc1+2
UAS-Rheb
F
S
F
S
F
S
Myc-Atg1
Tubulin
100
50
F
Myc-Atg1
UAS-Atg1$^{6B}$
UAS-Atg1$^{GS}$
F
S
F
S
F
S
Atg1
100

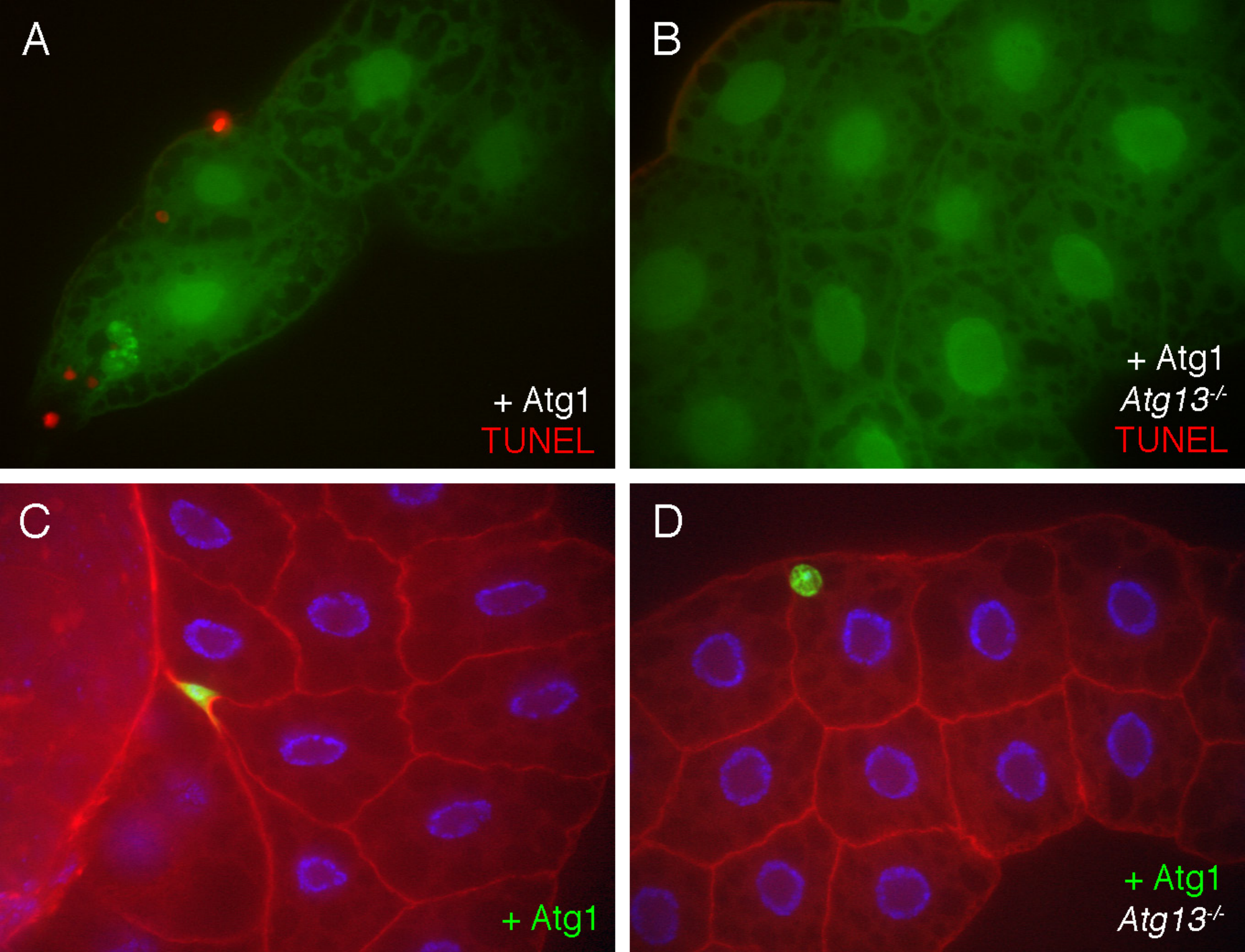
A
+ Atg1
TUNEL
B
+ Atg1
Atg13-/-
TUNEL
C
+ Atg1
D
+ Atg1
Atg13-/-